

# Research on Visual Detection Algorithm for Groove Feature Sizes by Means of Structured Light Projection

ZHA Anfei<sup>1</sup>, LU Yonghua<sup>1\*</sup>, WANG Mingxin<sup>2</sup>, ZHU Huayu<sup>1</sup>

1. College of Mechanical and Electrical Engineering, Nanjing University of Aeronautics and Astronautics, Nanjing 210016, P. R. China; 2. Nanjing Atekon Automation Technology Co., Ltd., Nanjing 210012, P. R. China

(Received 31 March 2021; revised 3 June 2021; accepted 11 June 2021)

**Abstract:** The visual inspection is an economical and effective method for welding. For measuring the feature sizes of grooves, a method based on line structured light is presented. Firstly, an adaptive algorithm to extract the sub-pixel centerline of structured light stripes is introduced to deal with the uneven width and grayscale distributions of laser stripes, which is based on the quadratic weighted grayscale centroid. By means of region-of-interest (ROI) division and image difference, an image preprocessing algorithm is developed for filtering noise and improving image quality. Furthermore, to acquire geometrical dimensions of various grooves and groove types precisely, the sub-pixel feature point extraction algorithm of grooves is designed. Finally, experimental results of feature size measuring show that the absolute error of measurement is 0.031—0.176 mm, and the relative error of measurement is 0.2%—3.6%.

**Key words:** groove measurement; line structured light; centerline extraction; feature point extraction

**CLC number:** TP242      **Document code:** A      **Article ID:** 1005-1120(2022)03-0367-12

## 0 Introduction

Welding is widely used in metal processing. The machine vision based on line structured light has the advantages of non-contact, high precision and quite high speed, and it is regarded as the most promising technology to detect the weld seams. The application of structured light in weld inspection originated in 1970s has made a series of achievements in recent years<sup>[1]</sup>. Han et al.<sup>[2]</sup> developed a structural light vision sensor with a narrow band filter, using the feature extraction algorithm of the filling weld bead and the capping weld bead for evaluating the weld quality. In order to realize real-time seam tracking of multi-layer and multi-pass welding, Zeng et al.<sup>[3]</sup> introduced a method that combines directional and structural light image to detect weld edge precisely. Based on structured light vision, Wang et al.<sup>[4]</sup> adopted ensemble learning mod-

els to recognize weld seam types, which include BP-Adaboost and KNN-Adaboost.

The mature commercial products of weld tracking and quality evaluation based on laser vision appeared in the United States, Denmark and Germany<sup>[5]</sup>. The Laser Tracking produced by ASEA Robotics in Denmark can accomplish the localization and tracking of different kinds of weld seams such as butt and corner joints, with the accuracy up to 0.4 mm<sup>[6]</sup>. The TH6D from Scansonic can complete more precise seam tracking by multiple light beams<sup>[7]</sup>. In 2012, the monitoring system of welding by means of laser vision came on the scene at Southern Methodist University, which can measure the 3D contour of weld joints and evaluate welding quality in real time<sup>[8]</sup>.

Achieving geometrical dimensions of welding grooves and recognizing groove types are important

\*Corresponding author, E-mail address: nuaa\_lyh@nuaa.edu.cn.

**How to cite this article:** ZHA Anfei, LU Yonghua, WANG Mingxin, et al. Research on visual detection algorithm for groove feature sizes by means of structured light projection[J]. Transactions of Nanjing University of Aeronautics and Astronautics, 2022, 39(3):367-378.

<http://dx.doi.org/10.16356/j.1005-1120.2022.03.011>

contents to weld inspection, which are key to the path planning of welding robots and the selection of material and welding parameters. According to the shape, the welding grooves are mainly classified into five types: Square groove, lap groove, single bevel groove, V-groove and U-groove<sup>[9]</sup>.

The centerline extraction of laser stripes and the feature point detection of grooves are two important parts of groove geometrical dimension measurement. The traditional methods for acquiring the laser stripe center are geometrical center extraction and energy center extraction<sup>[10]</sup>. The former has slow speed and low precision, in which the skeleton thinning algorithm is a typical example. In the latter, the gray centroid algorithm performs excellently for accuracy and poorly in anti-jamming capability, and the algorithm based on Hessian matrix takes much time<sup>[11]</sup>. The algorithm for centerline extraction introduced in this paper adapts to the uneven width of laser stripe excellently, and has good performance in accuracy, which is an improvement to the gray centroid algorithm. In addition, the application of linear convolution and image difference effectively abolishes the noise.

Template matching and the method based on image sharpness are two classic methods to detect the feature points of grooves, which cannot achieve corner points accurately because these methods focus on the local features of laser images<sup>[12]</sup>. Corner location and groove type recognition are combined to extract groove feature points, in which the rough feature point positioning is accomplished by corner location, and the geometric relationship between corner points and fitting centerlines is used for calculating sub-pixel coordinates.

A method for measuring geometrical dimensions of various grooves is present in this paper. In section 1, the inspection system is presented. Then the algorithm of extracting the centerline of structured light stripes is introduced in section 2. For dimension measurement and groove type identification, the feature point extraction is crucial, which is detailedly described in section 3. Experiments of

evaluating the performance of the algorithms mentioned above are introduced in section 4. Finally, conclusions are drawn in section 5.

## 1 Inspection System Description

The weld groove inspection platform is shown in Fig.1. It is composed of three parts: A line-structured light vision sensor, an industrial computer and a single axis robot. A line laser and an industrial camera are used to set up a line-structured light vision sensor. The workpiece is held on a table driven by a single axis robot. The industrial camera is a MER-132-30GC with 16 mm focal length and can capture the image with pixel number of  $1\,292 \times 964$ . The power and central wavelength of the laser are 100 mW and 650 nm, respectively.

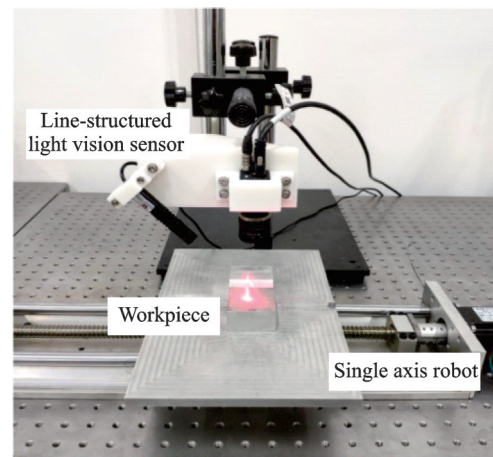


Fig.1 Hardware system for visual inspection

With the movement of the single axis robot, the sensor acquires 50 stripe images on different longitudinal sections of grooves to reduce random errors and increase the measurement reliability. The detection system gets 50 sets of measurements for each groove and the average is considered as the output value of geometrical sizes. The CPU frequency and RAM size of the industrial computer are 1.7 GHz and 4.0 GB, respectively. These algorithms introduced in this paper are written in C++ language on Visual Studio 2013 and the software toolkit for image processing is OpenCV 2.4.9.

## 2 Image Processing Algorithm for Extracting Centerline of Structured Light Stripes

To measure the feature size of grooves, it is a prerequisite to achieve the centerline of laser stripes. Traditional algorithms for extracting the laser stripe center include the skeleton thinning algorithm, the gray centroid algorithm and the algorithm based on Hessian matrix<sup>[13]</sup>. As shown in Fig.2, the width and gray distributions of laser stripes are uneven. An adaptive optimization algorithm for extracting the sub-pixel center of structured light stripes is proposed. According to the adaptive width quadratic weighted grayscale centroid algorithm, the initial stripe center points are obtained, after that the accurate center coordinates are achieved through making analysis of the slope threshold. Compared with the above three traditional algorithms, the accuracy of the proposed algorithm is improved by 28.1%, 58.2% and 12.9%, respectively.

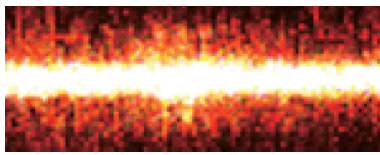


Fig.2 Image of a laser stripe

### 2.1 Adaptive width quadratic weighted grayscale centroid algorithm

(1) Edge detection of laser stripes

As shown in Fig.3, image pixels are scanned column by column from left to right and top to bottom until the first pixel  $P_l(x_l, y_l)$  with a gray value of 255 is searched at left side or the last pixel  $P_r(x_r, y_r)$  to the right. The pixels at the laser stripe are expressed by

$$\{f(x, y) | x_l \leq x \leq x_r, y_l \leq y \leq y_r\} \quad (1)$$

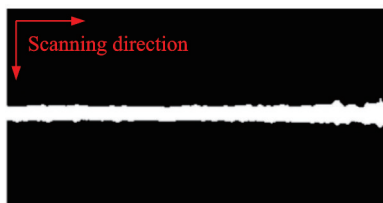


Fig.3 Image scanning

The width varies along the length of laser stripes, which can be computed by the longitudinal coordinate of upper and lower edges. The pixels in the  $i$ th section are expressed by

$$\{f_i(x, y) | y_{up}(i) \leq y(i) \leq y_{down}(i) = y_{up}(i) + w_i\} \quad (2)$$

where  $f_i(x, y)$  is the set of pixels at the  $i$ th section;  $y_{up}(i)$  and  $y_{down}(i)$  are the longitudinal coordinates of the upper and lower edges at the  $i$ th section, respectively;  $w_i$  is the width of the  $i$ th section that could be calculated by

$$w_i = y_{down}(i) - y_{up}(i) \quad (3)$$

(2) Adaptive extracting initial center points of laser stripes

For the gray centroid algorithm, noise has a serious negative impact on laser centerline extraction. As shown in Fig.4, the gray values in the central region of the stripe are high and change slightly, so the adaptive width quadratic weighted grayscale centroid algorithm is adopted to achieve the initial center point  $P_i^0$  which is at the  $i$ th section. Through the upper and lower edges of laser stripes, the noise is excluded from the computation, thus the performance of the algorithm will be upgraded to offer better capabilities for anti-interference.

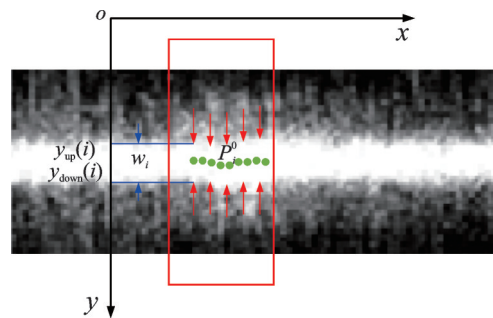


Fig.4 Schematic diagram of adaptive width quadratic weighted grayscale centroid algorithm

The  $y$ -coordinate of an initial center point,  $y_{center}^0(i)$ , can be calculated by

$$y_{center}^0(i) = \frac{\sum_{y=y_{up}(i)}^{y_{up}(i)+w_i} f_i^2(x, y) \cdot y}{\sum_{y=y_{up}(i)}^{y_{up}(i)+w_i} f_i^2(x, y)} \quad (4)$$

## 2.2 Optimized algorithm based on discrete analysis of center points

In order to improve the extraction accuracy of stripe center points and debase the influence of noise, an algorithm that optimizes the initial center points is designed based on making analysis of the slope threshold, in which the least square method is used to fit the experimental data. The optimization process of the initial center points is divided into two steps.

### (1) Mean optimization

The average of the initial center points in each window is computed as the optimized center point  $P_i^1(x, y_{\text{center}}^1(i))$  and the window centered on the initial point  $P_i^0$  slides from left to right with the size of  $a \times a$ . The value of  $y_{\text{center}}^1(i)$  can be calculated by

$$y_{\text{center}}^1(i) = \frac{\sum_{m=i-\frac{a-1}{2}}^{i+\frac{a+1}{2}} y_{\text{center}}^0(m) - y_{\text{center}}^0(i)}{a-1} \quad (5)$$

where  $i$  and  $m$  are the sequence numbers of section;  $y_{\text{center}}^0(i)$  and  $y_{\text{center}}^0(m)$  the  $y$ -coordinates of the initial center points at the  $i$ th and  $m$ th sections, respectively.  $y_{\text{center}}^1(i)$  is the  $y$ -coordinate of  $P_i^1$ ; and  $a$  is the side length of the window.

### (2) Analyzing dispersion and relocating center points

According to the border points  $P_l$  and  $P_r$  referred in Section 2.1, the slope threshold  $k_T$  is used to evaluate the dispersion of initial center points. It could be calculated by

$$k_T = \frac{y_r - y_l}{x_r - x_l} \quad (6)$$

where  $x_r$  and  $x_l$  are the  $x$ -coordinates of  $P_r$  and  $P_l$ , and  $y_r$  and  $y_l$  are the  $y$ -coordinates of  $P_r$  and  $P_l$ , respectively.

When the window slides along the optimized center points from left to right, the slope  $k_1$  between the center points  $P_i^1$  and  $P_{i-b}^1$  could be calculated by

$$k_1 = \frac{y_{\text{center}}^1(i) - y_{\text{center}}^1(i-b)}{b} \quad (7)$$

where  $y_{\text{center}}^1(i)$  is the  $y$ -coordinate of  $P_i^1$ ,  $i$  the sequence number of sections, and  $b$  the difference in the  $x$ -coordinate of two sections.

The algorithm determines whether the dispersion of the optimized center points exceeds standard by means of analyzing  $k_T$  and  $k_1$ . The relocation of  $P_i^1$  is necessary, if  $k_1$  is 10 times larger than  $k_T$ . The  $y$ -coordinate of the final center point  $P_i^2$  could be calculated by

$$y_{\text{center}}^2(i) = \begin{cases} y_{\text{center}}^1(i) & k_1 \leq 10k_T \\ y_{\text{center}}^1(i-b) + b \times k_T & k_1 > 10k_T \end{cases} \quad (8)$$

By all the above processes, the sub-pixel center point at the  $i$ th section is  $P_i^2$ .

## 3 Algorithm of Image Preprocessing and Feature Point Extraction for Laser Stripe on Grooves

As shown in Fig.5, the image preprocessing is completed firstly. Then after centerline extraction, feature points are extracted. Finally the feature sizes of grooves are calculated.

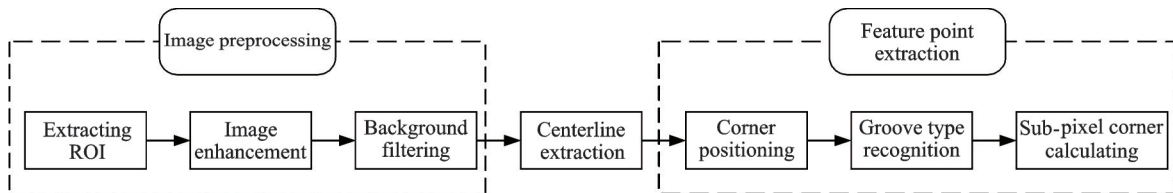


Fig.5 Flow chart of laser image processing

### 3.1 Image preprocessing

Image interferences near the laser stripe are ac-node noise and fuzzy flare as result of specular reflection and diffuse reflection on metallic surface. With the increasing of laser power, this phenomenon be-

comes more obvious. In addition, small speckle noise and solitary points are produced by the system hardware, such as laser devices and industrial cameras, because of the changes of anti-jamming capability.



## (1) Image enhancement

The automatic measurement of feature sizes must own satisfactory capability because it aims at five types of grooves. As shown in Fig.6, through the feature analysis of laser stripes on different kinds of grooves, the laser stripe is split into three parts: The left, middle and right laser regions. As a result, the computation load for the pretreatment process is reduced significantly. The template matching is one way to accomplish ROI division, but it needs a long time<sup>[14]</sup>. In this paper, the laser image is scanned from top to bottom, and the row with the maximum gray value is thought as the baseline. The pixels with the gray value less than 100 are searched from left to right along the baseline, and the pixels nearest to the laser stripe are the horizontal border points of ROI. The vertical borders of ROI are determined by the number of pixels with gray value of 255 at every row.

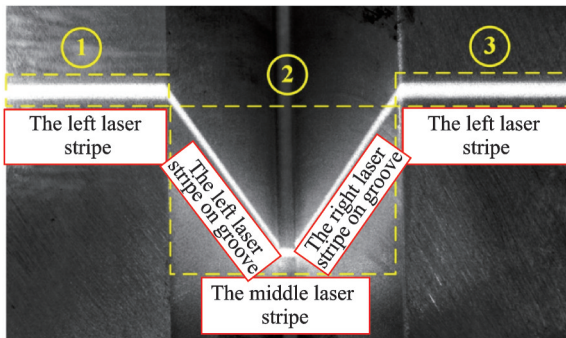


Fig.6 Division of laser stripes

The traditional image enhancement approaches are not good solutions to the problem of low contrast between the object and background in laser images. These approaches include histogram equalization, logarithmic transformation, gamma correction, Laplace operator and Wiener filtration<sup>[15]</sup>. An image enhancement algorithm based on linear convolution and image difference is proposed to improve the quality of the laser stripe in noise background.

There are elongated laser stripes extending horizontally in the left or right region where anisotropic scattered facula and acnode noise are found principally. For the above reason, laser images are enhanced in the horizontal direction. The convolution window

should be longer than the stripe with the width of 30—40 pixels in the experiment platform. The window size is set to  $41 \times 1$ .  $M_1^T$  is the revolution of the convolution window  $M_1$

$$M_1^T = [-1 \quad \dots \quad -1 \quad 40 \quad -1 \quad \dots \quad -1] \quad (9)$$

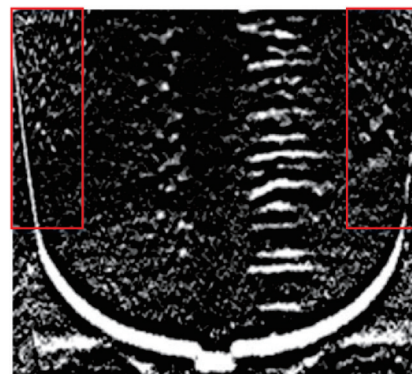
There is a small horizontal laser stripe with the width of about 30 pixels in the middle region, and the size of the convolution window is set to  $31 \times 1$ .  $M_2^T$  is the revolution of the convolution window  $M_2$

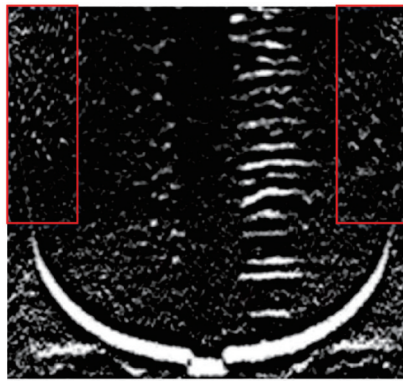
$$M_2^T = [-1 \quad \dots \quad -1 \quad 30 \quad -1 \quad \dots \quad -1] \quad (10)$$

The width of interference stripes is about 5 pixels. As shown in Eq.(11), the convolution window is  $M_3$ , whose size is set to  $1 \times 5$ .

$$M_3^T = [-1 \quad -1 \quad 4 \quad -1 \quad -1] \quad (11)$$

The difference image between laser images convoluted by  $M_1$  and  $M_3$  or between  $M_2$  and  $M_3$  is the result of image enhancement. As shown in Fig.7 (a), the laser stripes in red boxes are interference stripes, which are obvious after the convolution operation by  $M_3$  as shown in Fig.7(b). The difference image between laser images convoluted by  $M_2$  and  $M_3$  is shown in Fig.7(c), and the noise and interfer-

(a) Laser image convoluted by  $M_2$ (b) Laser image convoluted by  $M_3$



(c) Difference image between the laser images convoluted by  $M_2$  and  $M_3$

Fig.7 Process of image enhancement

ence stripes are suppressed considerably.

(2) Background filtering

In order to filter image background and extract intact stripes, the morphological opening is combined with connection area removal in this paper. For the binary image obtained by Otsu method, the larger grain noise is eliminated by morphological operation. Afterwards, connection areas are searched

to delete residual noise according to area-size features. Finally, stripe edges are smoothed by closing operation of mathematical morphology.

3.2 Sub-pixel feature point extraction algorithm of grooves

After laser stripe centerlines are gained, it is necessary to implement the type recognition and accurate corner extraction by the characteristics of various grooves.

As shown in Fig.8, the points  $A_c, B_c, C_c, D_c, E_c, F_c$  are general corner points because these points exist in every kind of groove, and the special corner points are points  $G_c, H_c, M_c, N_c$  because these points only appear on V-groove and U-groove. The characteristics of various grooves are summarized in Table 1 and the methods to find corner points are shown in Table 2. For example, in single bevel groove, points  $B_c$  and  $C_c$  have the same  $x$ -coordinate, but the  $x$ -coordinate of point  $D_c$  differs from that of point  $E_c$ .

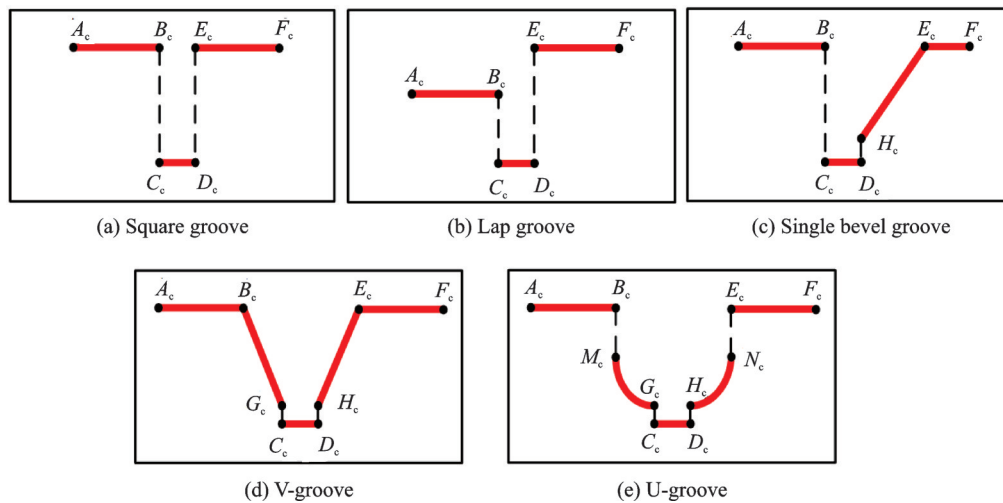


Fig.8 Characteristics of various types of grooves

Table 1 Characteristics of various grooves

Groove type	Characteristic
Square groove	$\Delta x_{BC} = \Delta x_{DE} = 0$
Lap groove	$ \Delta y_{AE}  > 0$
Single bevel groove	$\Delta x_{BC} = 0,  \Delta x_{DE}  > 0$
V-groove	$ \Delta x_{BC}  > 0,  \Delta x_{DE}  > 0$ , the slopes of curves $BG$ and $HE$ are invariable
U-groove	$ \Delta x_{BC}  > 0,  \Delta x_{DE}  > 0$ , points $M_c$ and $N_c$ appear, the slopes of curves $BG$ and $HE$ are variable

**Table 2** Methods for extracting corner points

Corner point	Extraction method
$A_c$	Column scanning image pixels from left to right and top to bottom until the first pixel with gray value of 255 is searched.
$F_c$	Column scanning image pixels from right to left and top to bottom until the first pixel with gray value of 255 is searched.
$C_c$	Column scanning image pixels from left to right and bottom to top until the first pixel with gray value of 255 is searched.
$D_c$	Column scanning image pixels from right to left and bottom to top until the first pixel with gray value of 255 is searched.
$B_c$	Searching image pixels at $A_c$ along laser stripe centerline from left to right until the first corner point is searched.
$E_c$	Searching image pixels at $F_c$ along laser stripe centerline from right to left until the first corner point is searched.
$G_c$	Scanning image pixels at $C_c$ from left to right and bottom to top until the first corner point is searched.
$H_c$	Scanning image pixels at $D_c$ from right to left and bottom to top until the first corner point is searched.
$M_c$	Scanning image pixels at $B_c$ from left to right and top to bottom until the first corner point is searched.
$N_c$	Scanning image pixels at $E_c$ from right to left and top to bottom until the first corner point is searched.

The general corner points are obtained by image scanning, after that the groove types can be recognized initially, then the special corner points of grooves are extracted in turn. By means of the slope and coordinate difference between corner points, the groove type recognition can be realized precisely.

After the groove type identification and rough corner positioning, it is necessary to carry out the sub-pixel coordinate extraction of groove feature points. According to the algorithm proposed in Section 2, laser stripe centerlines are achieved precisely, then the least-square method is used for fitting straight line  $l$ .

As shown in Fig.9, the sub-pixel coordinates of feature points are calculated by the straight-line intersection method and the minimum distance method. For extracting sub-pixel feature points, the first method finds intersection points between two lines and the last method calculates the foot point of an initial corner point to line. For example, the point  $B_f$  is the intersection point between the fitting centerlines  $l_1$  and  $l_2$  in V-groove, and the sub-pixel coordinate of  $B_f$  is computed by slope and intercept. In square groove, the point  $B_f$  is the foot point of  $B_c$  to  $l_1$ , which can be calculated according to the coordinate of  $B_c$ , the slope and intercept of  $l_1$ .

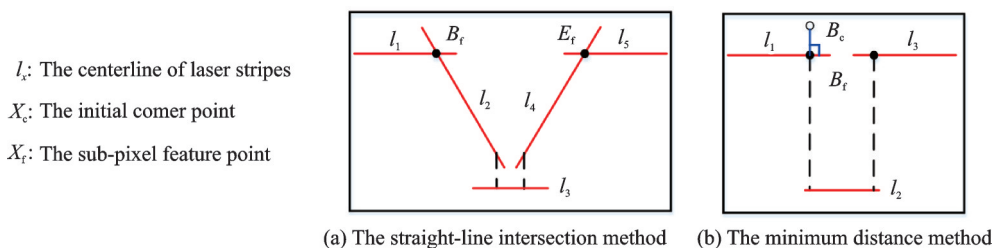


Fig.9 Schematic diagram of extracting sub-pixel feature points

## 4 Experimental Results and Analysis

### 4.1 Experimental comparisons and precision analysis of different center extraction algorithms

Different algorithms are adopted to verify the effectiveness of the optimized centerline extraction algorithm. After completing the preprocessing of laser images, the skeleton algorithm, the gray cen-

triod algorithm, the algorithm based on Hessian matrix and the algorithm introduced in this paper are used to achieve the center points of six laser images for each algorithm. The experimental data are analyzed by some evaluation indexes, such as standard deviation and repeatability.

The precision of the above algorithms is estimated by the standard deviation of the distance between center points and the fitting line. The ability of the algorithm to resist random noise is evaluated by repeatability error. Under the same working con-

dition, six images of laser stripes are captured, but the center points extracted from the first image are regarded as the reference.

The experiment results of different center ex-

traction algorithms are shown in Table 3. As can be seen from Table 3, the proposed algorithm achieves the greatest operating efficiency, the maximum accuracy, and the best repeatability.

**Table 3 Accuracy of the center point extraction by different algorithms**

Evaluation index	The skeleton thinning algorithm	The gray centroid algorithm	The algorithm based on Hessian matrix	The proposed algorithm
Accuracy grade	Pixel	Sub-pixel	Sub-pixel	Sub-pixel
Running time $t$ /ms	642	32	811	31
Standard deviation $\sigma$ /pixel	0.32	0.55	0.28	0.23
Repeatability error $E_r$ /pixel	0.037 7	0.204 6	0.061 7	0.019 8

#### 4.2 Experimental results and analysis of groove feature point extraction algorithms

Harris<sup>[16]</sup>, Shi-Tomasi<sup>[17]</sup> and the algorithm

based on sharpness<sup>[18]</sup> are applied for detecting the corner point of V-groove in the input image, which only contains the centerline of laser stripes. The parameters of three algorithms are shown in Table 4.

**Table 4 Parameters of different feature point extraction algorithms**

Corner detection algorithm	Coefficient of quality grade	Neighborhood	Tolerance minimum distance	Threshold of sharpness
Harris <sup>[16]</sup>	0.06	3		
Shi-Tomasi <sup>[17]</sup>	0.1		50	
The algorithm based on sharpness <sup>[18]</sup>		3		0.05

The Euclid distance between the actual corner points obtained by manual marking and the detected corner points are calculated. If the distance is less than 5 pixels, the corner extraction is a success, otherwise a failure. In order to evaluate the effect of corner detection in different algorithms for the laser strip center-

line, the error detection rate, the miss detection rate, the position error and running time are served as indexes. The position error is the average distance between correct corner points and manually marked corner points. The results of different corner detection algorithms for V-groove are shown in Table 5.

**Table 5 Experimental results of different corner detection algorithms**

Corner detection algorithm	Error detection rate /%	Miss detection rate /%	Position error / pixel	Running time /ms
Harris <sup>[16]</sup>	100	16.7	1.84	78
Shi-Tomasi <sup>[17]</sup>	100	66.7	2.08	452
The algorithm based on sharpness <sup>[18]</sup>	100	33.3	0.59	15
The proposed algorithm	0	0	0.50	31

The proposed corner detection algorithm is superior to the other three algorithms. The error detection rate and miss detection rate are zero, the corner position error is only 0.50 pixel and the running time is 31 ms. In conclusion, the algorithm has high accuracy and good real-time performance in corner detection.

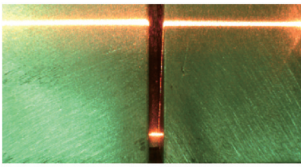
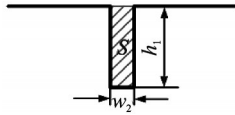
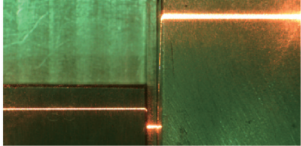
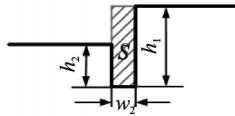
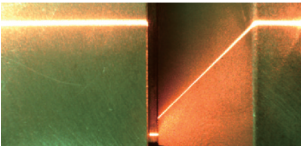
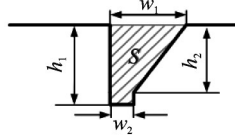

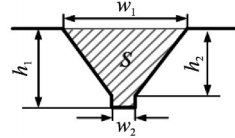

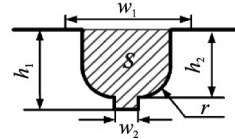
#### 4.3 Experimental results of feature size measuring of grooves

The feature sizes of various grooves are shown in Table 6.

In order to evaluate the performance of the method for feature size measuring of grooves, the measurement accuracy is analyzed. The accuracy re-



**Table 6 Feature sizes of various grooves to be measured**

Groove type	Images of laser stripes	Feature sizes to be measured
Square groove		
Lap groove		
Single bevel groove		
V-groove		
U-groove		

fers to the degree of numerical deviation between the output values and the truth values. In general, the absolute error and the relative error are used to estimate the accuracy of the system. The method of accuracy test is as follows.

(1) As shown in Fig.10, the ROMER Absolute Arm 7325 is applied to obtain the real feature sizes of various grooves, and its measurement accuracy is  $\pm 0.051$  mm at the range of 2.5 m. The true feature sizes are shown in Table 7.

(2) The sensor captures 50 laser images on different longitudinal sections of grooves and calculates 50 data values, and the average of these data is thought as the output values.

(3) The measurement values of each image and the output values are used to calculate the absolute error and relative error respectively.

As shown in Fig.11, the vertical and horizontal coordinates are the absolute error of each image and the sequence number of images, respectively. The



Fig.10 Approach for obtaining truth values of feature sizes

**Table 7 True values of feature sizes**

Groove type	$w_1$ /mm	$w_2$ /mm	$h_1$ /mm	$h_2$ /mm	$r$ /mm
Square groove		2.057	20.193		
Lap groove		2.070	20.099	3.955	
Single bevel groove	15.895	2.040	20.161	16.616	
V-groove	23.202	2.032	20.244	19.095	
U-groove	19.442	2.040	20.114	19.284	9.912

absolute error of the detection system is 0.031—0.176 mm, and the relative error is 0.2%—3.6%, indicating the effectiveness of the proposed algorithm. The above results are shown in Fig.11 and Table 8.

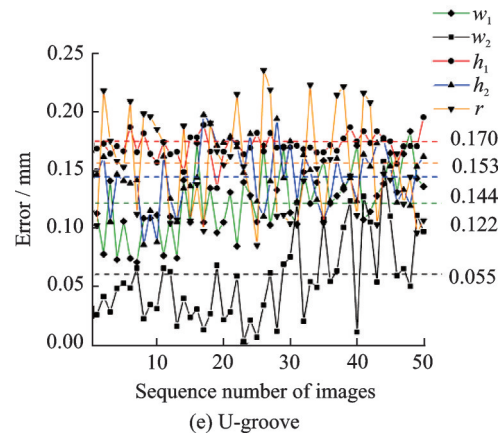
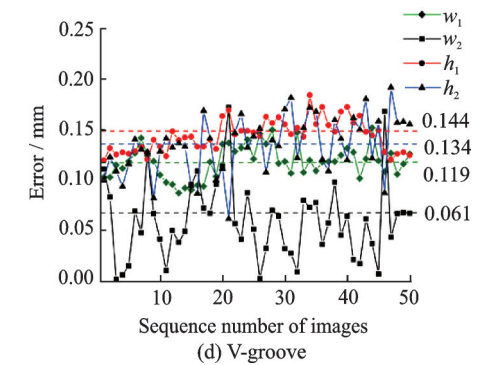
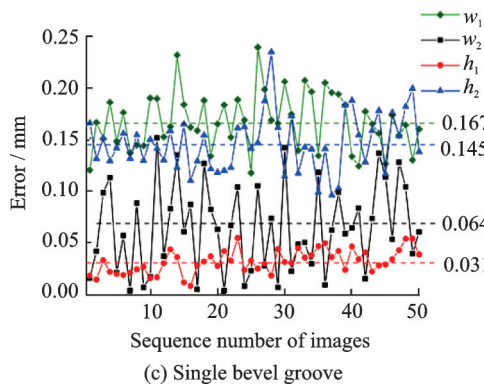
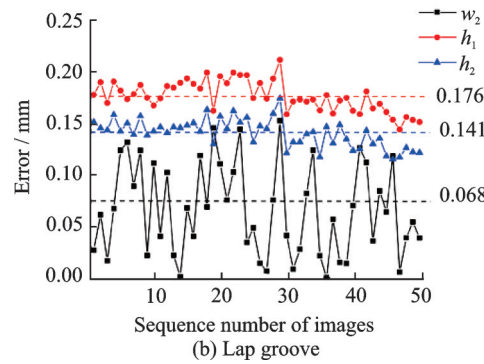
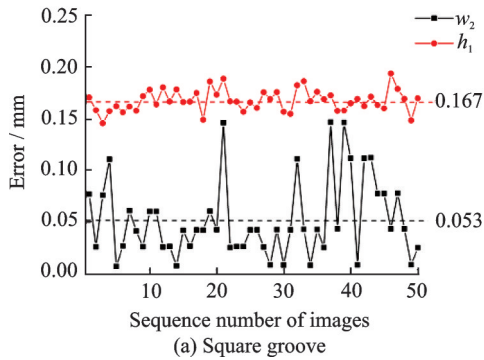


Fig.11 Scatter plots of the system absolute error on different grooves

**Table 8 The relative error of feature sizes** %

Groove type	$w_1$	$w_2$	$h_1$	$h_2$	$r$
Square groove		2.6	1.2		
Lap groove		3.3	0.9	3.6	
Single bevel groove	1.1	3.1	0.2	0.9	
V-groove	0.5	3.0	0.7	0.7	
U-groove	0.6	2.7	0.9	0.8	1.8

The main reasons for the above error performance are as follows:

(1) The image quality of various grooves is different, and the line structured light stripe sometimes cannot accurately display the complete morphology of grooves. It is easy for laser stripes on the square groove, the lap groove and the single bevel groove to be covered, so the output values differ from the truth values to a greater degree.

(2) Groove samples cannot be processed at high precision. That leads to the difference between section geometry sizes and it has bad impact on the consistency of measurement results.

(3) The stability of hardware affects the measurement accuracy of geometrical dimensions, such as the change in laser power.

(4) This paper adopts the image difference and feature point extraction algorithms, which may affect the measurement accuracy of geometrical dimension. The anti-interference performance of these algorithms is not very good and some implementation steps need to be further improved.

## 5 Conclusions

A method based on machine vision for detecting groove feature sizes is proposed. The algorithms of sub-pixel centerline extraction, image preprocessing, corner extraction are introduced in detail. In particular, some conclusions are reached as follows:

(1) The centerline extraction algorithm includes the adaptive width quadratic weighted grayscale centroid algorithm and optimized relocation algorithm. The effect of centerline extraction is wonderful.

(2) The image preprocessing combines image enhancement and background filtering, and the image quality of laser stripes is greatly improved.

(3) The corner extraction algorithm fuses type recognition and corner extraction, so the sub-pixel coordinates of corners can be achieved precisely.

(4) For the system used to measure groove feature sizes, the absolute error is 0.031—0.176 mm, and the relative error is 0.2%—3.6%. It shows that the algorithms of the system are quite effective and practicable.

According to the high accuracy of the detection system, the algorithms for measuring the groove feature size in this paper are proved a success.

## References

- [1] WILL P M, PENNINGTON K S. Grid coding: A preprocessing technique for robot and machine vision[J]. *Artificial Intelligence*, 1971, 2(3/4): 319-329.
- [2] HAN Y, FAN J, YANG X. A structured light vision sensor for on-line weld bead measurement and weld quality inspection[J]. *The International Journal of Advanced Manufacturing Technology*, 2020, 106(5): 2065-2078.
- [3] ZENG J, CHANG B, DU D, et al. A weld position recognition method based on directional and structured light information fusion in multi-layer/multi-pass welding[J]. *Sensors*, 2018. DOI: 10.3390/s18010129.
- [4] WANG Z, JING F, FAN J. Weld seam type recognition system based on structured light vision and ensemble learning[C]//*Proceedings of 2018 IEEE International Conference on Mechatronics and Automation (ICMA)*. [S.l.]: IEEE, 2018: 866-871.
- [5] ROUT A, DEEPAK B B V L, BISWAL B B. Advances in weld seam tracking techniques for robotic welding: A review[J]. *Robotics and Computer-Integrated Manufacturing*, 2019, 56: 12-37.
- [6] SICARD P, LEVINE M D. An approach to an expert robot welding system[J]. *IEEE Transactions on Systems, Man, and Cybernetics*, 1988, 18(2): 204-222.
- [7] WANG N, ZHONG K, SHI X, et al. A robust weld seam recognition method under heavy noise based on structured-light vision[J]. *Robotics and Computer-Integrated Manufacturing*, 2020, 61: 101821.
- [8] HUANG W, KOVACEVIC R. Development of a real-time laser-based machine vision system to monitor and control welding processes[J]. *The International Journal of Advanced Manufacturing Technology*, 2012, 63(1/2/3/4): 235-248.
- [9] TIAN Y, LIU H, LI L, et al. Automatic identification of multi-type weld seam based on vision sensor with silhouette-mapping[J]. *IEEE Sensors Journal*, 2020. DOI: 10.1109/JSEN.2020.3034382.
- [10] WANG Zehao, ZHANG Zhongwei. Adaptive direction template method to extract the center of structured light[J]. *Laser Journal*, 2017, 38(1): 60-64. (in Chinese)
- [11] WU X, TANG N, LIU B, et al. A novel high precise laser 3D profile scanning method with flexible calibration[J]. *Optics and Lasers in Engineering*, 2020, 132: 105938.
- [12] YE Z, PEI Y, SHI J. An improved algorithm for Harris corner detection[C]//*Proceedings of 2009 2nd International Congress on Image and Signal Processing*. [S.l.]: IEEE, 2009: 1-4.
- [13] LI Y, ZHOU J, HUANG F, et al. An improved gray weighted method for sub-pixel center extraction of structured light stripe[C]//*Proceedings of 2016 10th International Conference on Sensing Technology (IC-ST)*. [S.l.]: IEEE, 2016: 1-4.
- [14] YANG Xuejun, XU Yanling, HUANG Seji, et al. A recognition algorithm for feature points of V-groove welds based on structured light[J]. *Journal of Shanghai Jiaotong University*, 2016, 50(10): 1573-1577. (in Chinese)
- [15] SENGE N, SENGE A, CHOI H K. Image contrast enhancement using bi-histogram equalization with neighborhood metrics[J]. *IEEE Transactions on Consumer Electronics*, 2010, 56(4): 2727-2734.
- [16] HARRIS C, STEPHENS M. A combined corner and edge detector [C]//*Alvey Vision Conference 1988 Computer Science*. [S.l.]: [s.n.], 1988.
- [17] SHI J, TOMASI C. Good features to track [C]//*1994 Proceedings of IEEE Conference on Computer Vision and Pattern Recognition*. [S.l.]: IEEE, 1994.
- [18] QIAN Wenguang, LIN Xiaozhu. Detection algorithm

of image corner based on contour sharp degree [J]. Computer Engineering, 2008, 34 (6) : 202-204. (in Chinese)

**Acknowledgements** This work was supported by the National Natural Science Foundation of China (No. 51975293) and the Aeronautical Science Foundation of China (No. 2019ZD052010).

**Authors** Mr. ZHA Anfei received his B.S. degree and M.S. degree in mechanical engineering and mechatronic engineering from China University of Mining and Technology and Nanjing University of Aeronautics and Astronautics (NUAA) in 2019 and 2022, respectively. His research interests focus on machine vision, including linear structured light measurement, scratch inspection and optical character recognition.

Prof. LU Yonghua received Ph.D. degree in mechatronic en-

gineering from NUAA, Nanjing, China, in 2005. Now he is a full professor of College of Mechanical and Electrical Engineering, NUAA. His research interests focus on machine vision, photoelectric detection and robotics.

**Author contributions** Mr. ZHA Anfei designed the weld groove inspection system and algorithms, analyzed the experimental results and wrote the manuscript. Prof. LU Yonghua proposed the research topic, gave tips and supported on schematic design, paper writing and experimental analysis. Mr. WANG Mingxin provided experimental data, collected and arranged documents. Mr. ZHU Huayu participated in the algorithm design and coding, and experimental analysis. All authors commented on the manuscript draft and approved the submission.

**Competing interests** The authors declare no competing interests.

(Production Editor: WANG Jing)

## 基于线结构光的坡口特征尺寸检测算法研究

查安飞<sup>1</sup>, 陆永华<sup>1</sup>, 王明昕<sup>2</sup>, 朱华煜<sup>1</sup>

(1. 南京航空航天大学机电学院, 南京 210016, 中国; 2. 南京傲拓自动化技术有限公司, 南京 210012, 中国)

**摘要:** 机器视觉经济高效, 在焊缝检测中得到广泛的应用。基于线结构光技术, 本文提出一种坡口特征尺寸检测方法。首先, 针对激光光条灰度和宽度分布不均的问题, 介绍了一种基于二次加权灰度重心法的自适应中心线提取算法。其次, 为滤除图像噪声, 设计了一种基于感兴趣区域划分和图像差分的预处理算法。接着, 本文提出了一种亚像素特征点提取算法以计算坡口特征尺寸并识别坡口类型。最后, 实验结果表明, 坡口特征尺寸检测的绝对误差为 0.031~0.176 mm, 相对误差为 0.2%~3.6%。

**关键词:** 坡口检测; 线结构光; 中心线提取; 特征点提取